Available online at www.springerlink.com

Acta Metall. Sin. (Engl. Lett.) Vol.26 No.3 pp. 333—339 June 2013

ACTA
METALLURGICA SINICA
(ENGLISH LETTERS)

Prediction of the Residual Welding Stress in 2.25Cr-1Mo Steel by Taking into Account the Effect of the Solid-State Phase Transformations

Dean DENG[1,2)†], *Yangang TONG*[1)], *Ninshu MA*[3)] *and Hidekazu MURAKAWA*[3)]

1) College of Materials Science and Engineering, Chongqing University, Chongqing 400045, China

2) State Key Laboratory of Advanced Welding and Joining, Harbin Institute of Technology, Harbin 150001, China

3) JWRI, Osaka University, 11-1, Mihogaoka, Ibaraki, Osaka 567-0047, Japan

[Manuscript received 17 September 2012, in revised form 16 January 2013]

A computational approach based on the thermal elastic plastic finite element method was developed for predicting welding residual stress in low carbon alloyed steel welds by taking into account the effect of the solid-state phase transformations. The kinetics of phase transformations was described by Johnson Mehl Avrami Kolmogrov (JMAK) equation for bainitic transition and by Koistinen-Marburger (K-M) relationship for martensitic transition. Moreover, an additive rule depending on volumetric phase fraction was adopted to represent the material property changes during heating and cooling. Consequently, the residual welding stresses in a 2.25Cr1Mo steel TIG welded plate were computed. Early calculation results suggest that the bainitic and martensitic transformations took place in the weld the heat-affected zone drastically reduce the residual longitudinal tensile stress in the region.

KEY WORDS: Computational approach; Numerical simulation; Phase transformation; Welding residual stress

1. Introduction

It has been recognized that the solid-state phase transformation can significantly affect the profile of the residual stress in certain carbon alloyed steel weldments[1−3]. There are two main factors influencing on welding residual stresses. One is the shape deformation resulted form dilatational strain and shear strain; the other is the variation of the material properties such as the yield strength[4−6] or the plasticity induced by phase transformation[7−9].

In the past decades, a number of numerical models have been proposed to simulate residual stresses generated in weldments or heat treated structures by taking into account the effect of martensitic transformation[3]. However, researches that shone light on the effect of both bainitic and martensitic transformations using three-dimension finite element methods have not been forthcoming.

On the basis of thermal elastic plastic finite element method developed by joining and welding research institute (JWRI) of Osaka University[9,10], a new computational approach that takes into account the effect of both bainitic and martensitic transformations on residual welding stress was put forward. By using Johnson Mehl Avrami Kolmogrov (JMAK) equation to describe the bainitic transition and Koistinen-Marburger (K-M) relationship to trace the martensitic transition, the variation of material properties due to volumetric phase fraction changes during heating and cooling and its consequent effect on residual welding stresses were thoroughly examined.

2. Computational Approach

2.1 Thermo-metallurgical-mechanical finite element method

The computational procedure includes two steps.

† Corresponding author. Prof., Ph.D.; Tel: +86 23 65127340; Fax:+86 23 65112611; E-mail address: deandeng@cqu.edu.cn (Dean DENG)

DOI: 10.1007/s40195-012-0163-8

First, the temperature field and thermal cycle of each node is computed according to the welding heat input. Second, the microstructure, strain and stress are calculated upon the results of the first step. In the current work, the emphasis was laid on developing a series of subroutines to take into account the influence of solid-state phase transformation on strain/stress formation.

The kinetics of phase transformations was described by Johnson Mehl Avrami Kolmogrov (JMAK) equation for bainitic transition and by Koistinen-Marburger (K-M) relationship for martensitic transition. As shown in Fig. 1[11], the coupling effects among time, temperature filed, microstructure and stress/strain are very complex. It should be pointed out that factors such as the heat generated by plastic deformation, the latent heat due to solid-state phase transformation and the effect of stress on phase transformation were neglected.

2.2 A simple mixture rule to represent the variation of material properties

To investigate how the solid-state phase transformations affect residual welding stress, the variations of the volumetric phase fraction during the entire temperature range of phase transformation must be calculated beforehand. Then, the material properties such as the yield strength and the thermal expansion coefficient are estimated using a simple-mixture rule relating to volumetric phase fractions. The simple mixture rule is schematically shown in Fig. 2, in which only two phases (phase 1 and phase 2) are considered.

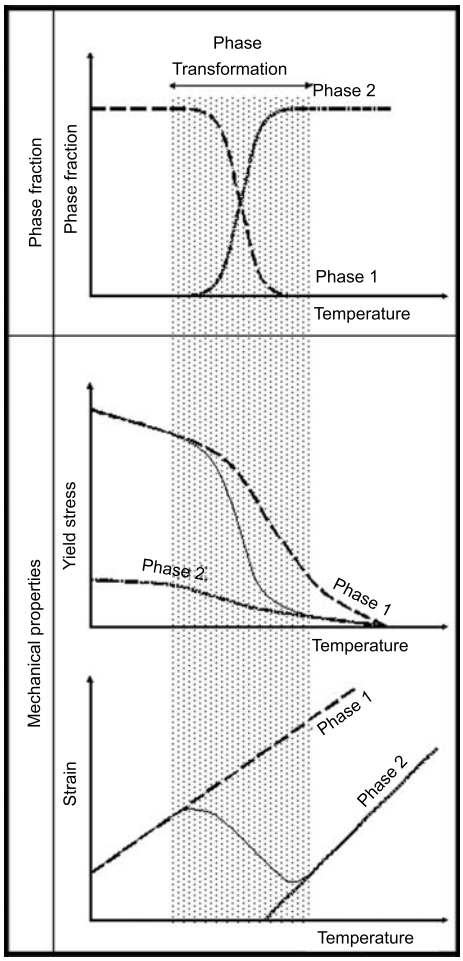

Fig. 2 Simple-mixture rule for considering materials property change during phase transformation

3. Algorithm of Phase Fraction

The chemical composition (wt.%) of 2.25Cr-1Mo steel is C 0.12, Si 0.26, Mn 0.48, Ni 0.08, Cr 2.00, Mo 0.96, V 0.08, Al 0.014 and Fe balanced. An entire welding thermal cycle includes a heating stage and a cooling stage. When the peak temperature is higher than A_1 (cementite disappearance temperature), the original phase starts to transform into austenite, and when temperature reaches A_3 (α-ferrite disappearance temperature), the original phases completely transform into austenite. For carbon alloyed steels, the original crystallographic structure of the base material should be body centered cubic (bcc) structure, so when these original phases change into austenite with a face centered cubic (fcc) structure the volume of the transformed material will decrease. Meanwhile, the material properties especially the mechanical properties will change greatly after austenitization.

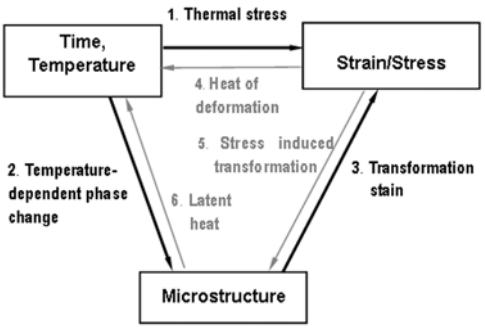

Fig. 1 The coupling of temperature, stress and microstructure[11]

According to the CCT diagrams of 2.25Cr-1Mo steel as shown in Fig. 3[12], austenite will transform into bainite and martensite during cooling stage. When the cooling rate is fast enough, austenite can fully transform into martensite, and when the cooling rate is moderate, it will transform into bainite and martensite.

The heat inputs generated by TIG welding processes usually result in a moderate cooling speed, so the austenite will decompose into a mixture of micro-structure consists of bainite and martensite.

3.1 Phase transition on heating

On heating, the level rule can be used to describe how the original phase changes into austenite. However, because the materials properties such as the

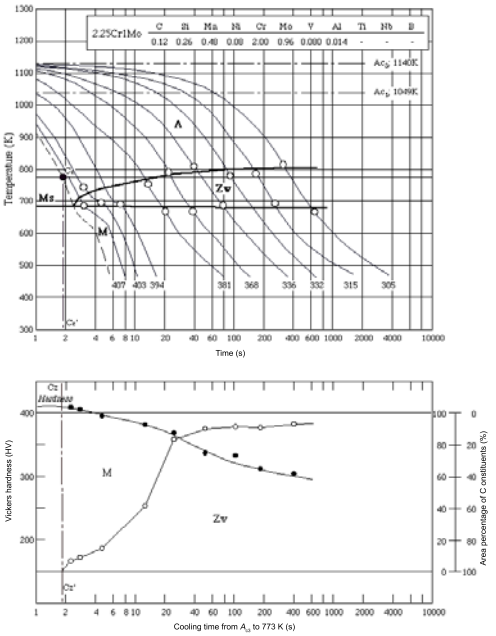

Fig. 3 CCT diagram of 2.25Cr-1Mo steel [12]

yield strength and Young′s modulus are relatively low when the temperature is higher than A_1 (the eutectoid temperature), it can be inferred that the phase transformation during heating would have little influence on the stress evolution. Therefore, for the sake of simplicity, a linear relationship is assumed to simulate the formation of austenite in the current study. By using the linear approximation, the austenite volume fraction (f_a) at each step can be calculated using the following equation.

$$f_a = \frac{T - T_1}{A_3 - A_1} \times 100\% \tag{1}$$

where T is the current temperature. A_1 and A_3 are assumed to be 770 °C and 880 °C, respectively.

3.2 Phase transformation during cooling

The computational procedures of solid-state phase transformation in 2.25Cr-1Mo steel during cooling stage can be schematically shown by Fig. 4, whilst Fig. 5 shows how austenite changes into bainite (phase A) and martensite (phase B).

3.2.1 Bainite transformation

In the past, several approaches such as regression model, thermo-dynamic and kinetic model and model based on CCT diagram have been used to predict micro-structures formation during welding. In the current study, an overall phase transformation theory is employed to predict phase transformation, in which the JAMK equation is employed to simulate austenite-bainite transformation. The parameters $k$and n of JMAK equation (see Eq. (2)) should be determined according to CCT diagram beforehand.

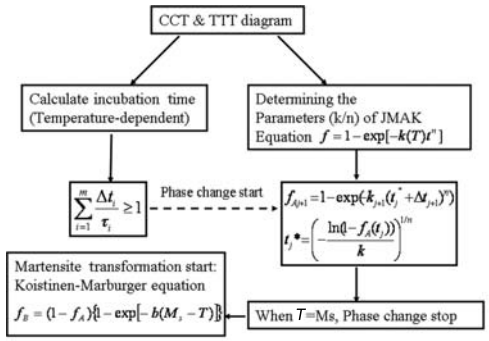

Fig. 4 Computational approach for modeling phase transformations during cooling in 2.25Cr-1Mo steel

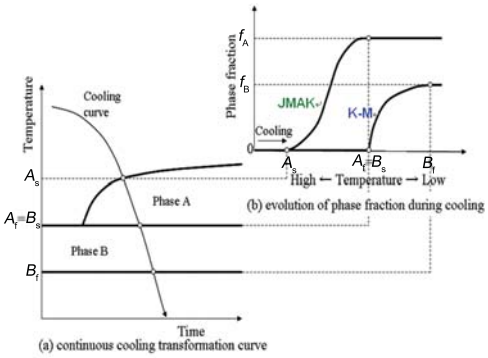

Fig. 5 Details of phase transformations during cooling stage

$$f = 1 - \exp(-kt^n) \tag{2}$$

The method proposed by Oliver[13] and CCT diagram from NIMS homepage[12] were used to determine the parameters k and n. It should be noted that the austenization temperature of 2.25Cr-1Mo steel is 1350 °C.

Fig. 6 shows the relationship between parameter n and the temperature. It can be seen that parameter n weakly depends on the temperature and n can be approximately taken as a constant (0.95). Fig. 7 shows the relationship between parameter k and temperature. It indicates that parameter k changes closely with temperature. A Gaussian distribution function was used to smoothly fit the relationship between parameter $k$and temperature in the present study.

Generally, there are two methods to track the evolution of bainite transformation during a non-isothermal diffusive transformation. One is to integrate the rate form of JMAK equation[14], and the other is to use Scheul′s additive rule. In the present numerical model, the latter method was used.

According to Scheul′s additive rule, a cooling curve can be subdivided into a series of small time steps (Δt). In each small step (Δt), the temperature can be taken as a constant. Here, let $f_{A,i-1}$be the vol-

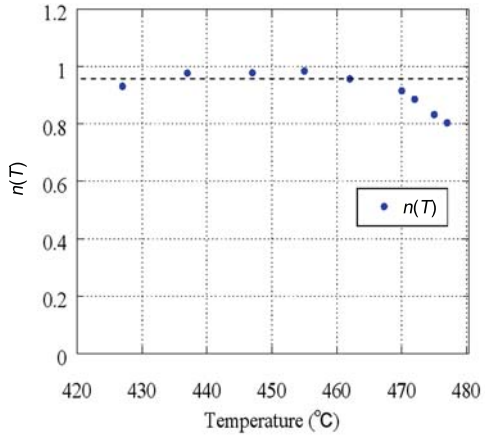

Fig. 6 Relationship between parameter n and the temperature

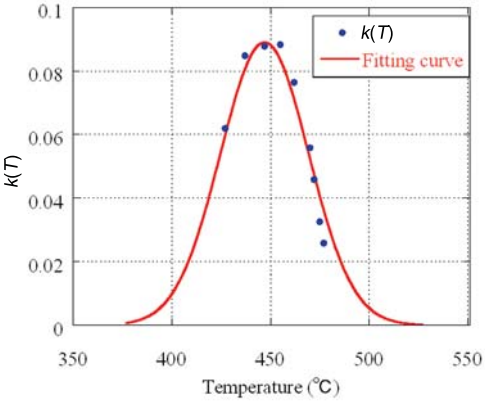

Fig. 7 Relationship between parameter k and the temperature

ume fraction of phase A transformed from austenite at the end of the $(i-1)$th step, and it is taken as the initial volume fraction of phase A for the next step (ith step). The fraction at the end of the ith step is determined by the following equation:

$$f_{\mathrm{A,i}} = 1 - \exp[-k_i t_i^n] \tag{3}$$

In the above equation, the t_i is given by the following formulation.

$$t_i = \Delta t_i + t_{i-1}^* = \Delta t_i + \left(-\frac{\ln(1-f_{A,i-1})}{k_i}\right)^{1/n} \tag{4}$$

where, Δt_i is the time increment of the ith step, t_{i-1}^* is a fictitious time[14] needed to obtain $f_{\mathrm{A},i-1}$ during the isothermal transformation at temperature T_i.

In the current numerical model, phase A is assumed to start to form when the following condition is fulfilled[4]:

$$\sum_{i=1}^{m} \frac{\Delta t_i}{\tau_i} \geq 1 \tag{5}$$

where τ_i is incubation time at the ith time step.

3.2.2 Martensite transformation

Koistinen-Marburger (K-M)[15] relationship is often used to describe the formation of martensite. In the current study, the volumetric fraction of martensite is determined by a modified K-M relationship[2].

$$f_{\mathrm{B}} = (1-f_{\mathrm{A}}) f_{\mathrm{mod}} \{1 - \exp[-b(M_{\mathrm{s}} - T)]\} \, (T \leq M_{\mathrm{s}}) \tag{6}$$

where f_{B} is the fraction of martensite (Phase B) at the current temperature (T); f_{A} is the fraction of bainite (Phase A); T is the current temperature; M_{s} is the start temperature of martensite, and b is a constant which represents the evolution of martensite transformation process. For carbon steel and low alloy steel, the value of b is 0.011[15]. It should be noted that f_{mod} is a modified coefficient, and it can be determined by the following formulation[2].

$$f_{\mathrm{mod}} = 1/\{1 - \exp\lfloor -b(M_{\mathrm{s}} - M_{\mathrm{f}})\rfloor\} \tag{7}$$

where, M_{f} is the finish temperature of martensite.

In the finite element model, the differential equation derived from Eq. (5) can be used to calculate the increment of martensite fraction at each step. For example, the increment of martensite fraction ($\Delta f_{\mathrm{B},j}$) at the jth step can be expressed as follows:

$$\Delta f_{\mathrm{B},j} = (1-f_{\mathrm{A}}) f_{\mathrm{mod}} \{-0.011 \exp[-0.011(M_{\mathrm{s}} - T)]\} \Delta T_{\mathrm{j}} \tag{8}$$

where, ΔT_j is the temperature increment at the jth step.

4. Predicting Residual Welding Stresses in a Bead-on-Plate Welded by TIG Welding Process

4.1 Finite element model

The finite element model for a workpiece in sizes of 200 mm×200 mm×3 mm is shown in Fig. 8. In this model, the number of element is 12160, and that of node is 15795. The welding conditions for the TIG welding process were assumed as follows: welding current was 150 A; arc voltage was 17 V; and welding speed was 5 mm/s. The arc coefficient was assumed to be 0.7.

A moving heat source with uniform density flux was used to model the heat input generated by TIG welding process. Meanwhile, the temperature-dependent thermal properties[16] were used to calculate the heat transfer in the finite element. Moreover, heat loss due to convection was considered using Newton′s law, and heat loss caused by radiation using Stefan-Boltzman′s law[11].

The elastic behavior was modeled using the isotropic Hook′s law, and the thermal strain

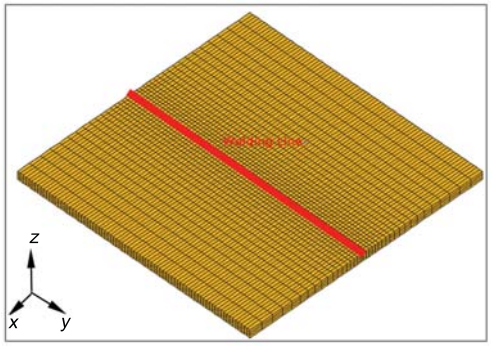

Fig. 8 Finite element model

was calculated using thermal expansion coefficient. For plastic behavior, a rate-independent plastic model was employed and the yield criterion is the Von Mises critirion. The temperature-dependent mechanical properties such as Young′s modulus and Possion′s ratio[16] were used in the mechanical analysis. Meanwhile, the volume change and the yield strength variation due to phase transformation were taken into account through using phase- temperature-dependent thermal expansion coefficient and yield strength, respectively. It was assumed that the volumetric strain due to either full martensite or full bainite transformation is 0.8% for 2.25Cr-1Mo steel[16]. The yield strength of each phase is shown in Fig. 9. A linear mixture rule was used to determine the yield strength ($\sigma_{\rm y}$) according to the volume fraction of each phase. The simple mixture rule can be expressed using the following formulation.

$$\sigma_{\rm y} = \sum_{i=1}^{n} \sigma_{{\rm y},i} f_i (i = 1, n) \tag{9}$$

where, $\sigma_{{\rm y},i}$ is the yield strength of phase i, and f_i is the fraction of phase i.

To clarify the influence of solid-state phase transformation on the welding residual stress, two cases (Case-1 and Case-2) were studied. Case-1 considered solid-state phase transformation, while Case-2 neglected this effect. In Case-2, the temperature-dependent thermal and mechanical properties of the initial phase were used in the entire thermal cycle. For example, the temperature-dependent yield strength is shown in Fig. 9(a).

4.2 Simulated results

Fig. 10 shows the maximum temperature distribution. This figure can help us to judge where the solid-state phase transition occurred. Fig. 11 shows distribution of each phase on the upper and bottom surfaces of the middle section. These figures tell us that the microstructure consists of bainite and martensite in weld zone and full heat-affected zone (HAZ). In the partial HAZ, the microstructure is a mixture consisting of initial phase, bainite and martensite. To

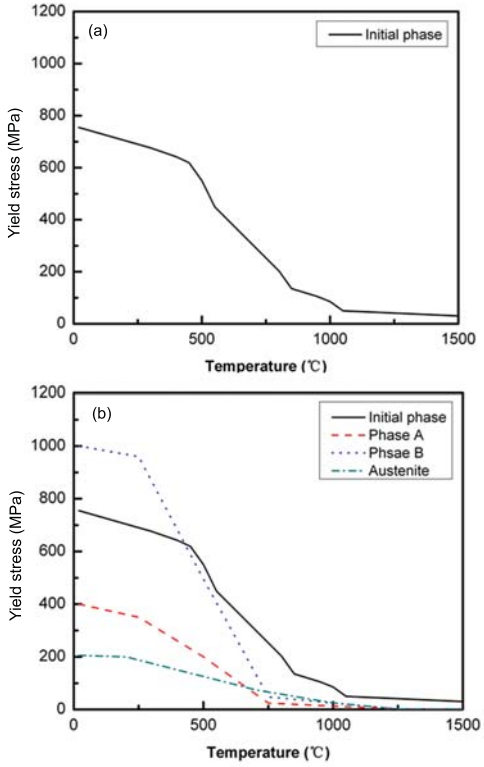

Fig. 9 Temperature-dependent yield strengths used in FE model: (a) yield strength without considering phase change; (b) yield strengths with considering phase change

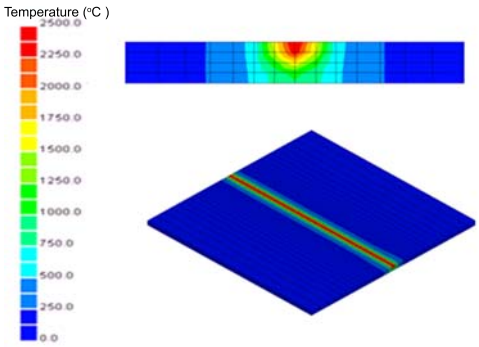

Fig. 10 Peak temperature distribution

carefully compare the welding residual stresses predicted by Case-1 and Case-2, we plotted the longitudinal residual stress distributions on the upper and bottom surfaces of the middle section in Fig. 12 and Fig. 13, respectively. From Fig. 12, we can know that the longitudinal residual stress values near the weld zone predicted by Case-1 are much smaller than those predicted by Case-2. In Case-1, because the volumetric change due to phase transformation was taken in account, the cumulated stress was partially or fully cancelled during the solid-state phase transformation. In Case-2the effect of phase transformation was neglected, so it is not strange that very large tensile residual stresses generated near the weld zone after welding. In Case-1, because the maximum temperature of the bottom surface is lower than that of the

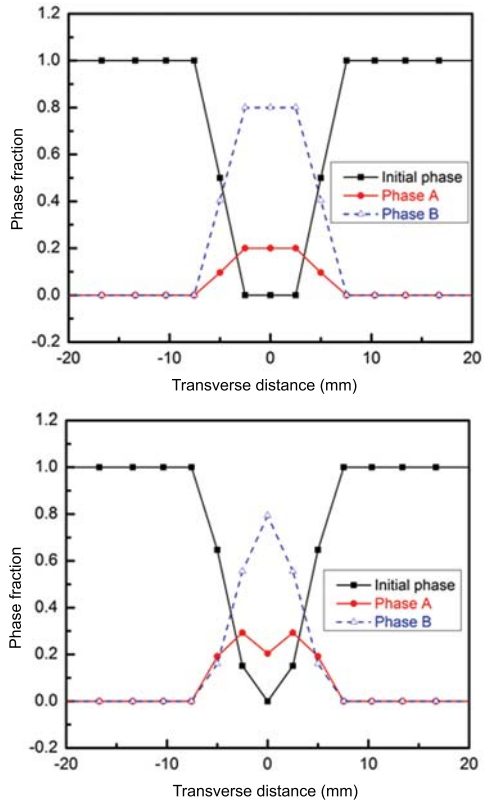

Fig. 11 Distribution of each phase fraction in the middle section: (a) upper surface; (b) bottom surface

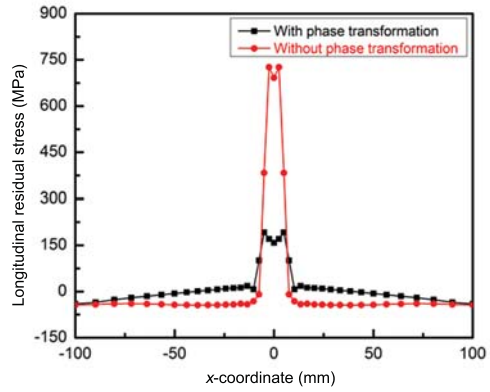

Fig. 12 Longitudinal residual stress distribution on the upper surface

upper surface, the range experienced the solid-state phase transformation is correspondingly smaller than that on the upper surface. This explains why relatively tensile residual stresses generated near the weld zone on the bottom surface. However, compared with Case-2, the peak tensile stress of Case-1 is lower.

Fig. 14 and Fig. 15 compare the transverse residual stress distributions of two cases on the upper and bottom surfaces of the middle section, respectively. Contrary to longitudinal stress, the transverse residual stresses near the weld zone in Case-1 are higher than those in Case-2. However, since the peak value of

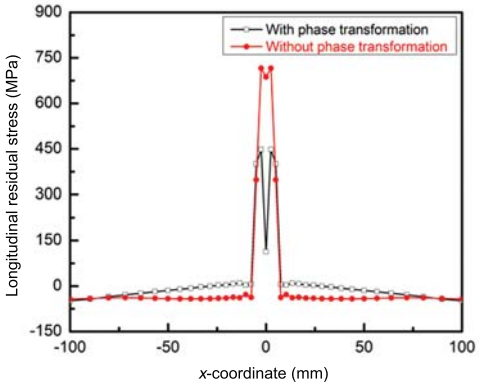

Fig. 13 Longitudinal residual stress distribution on the bottom surface

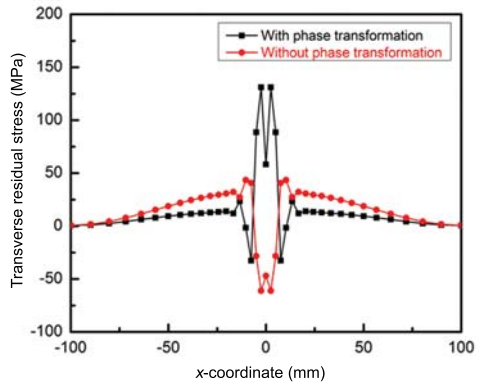

Fig. 14 Transverse residual stress distribution on the upper surface

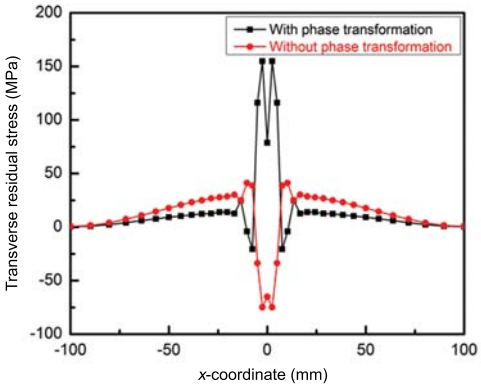

Fig. 15 Transverse residual stress distribution on the bottom surface

the residual tensile transverse stress is far lower than the yield strength of the material at room temperature, the adverse effect of such increase is largely compensated by the sharp drop in the longitudinal stress which is often regarded as unfavorable because its values are likely close or equal to the yield strength of the material. From Fig. 14 and Fig. 15, we can find that the solid-state phase transformation not only changed the value magnitude of transverse residual stress but also altered its value sign from negative (*i.e.* compressive) to positive (*i.e.* tensile) near the weld zone.

Further work combining the residual stresses with local damage and fracture mechanics and concerning a wider range of materials is worthwhile and has been underway.

5. Conclusions and Future Works

In the present work, a new computational approach to predict welding residual stresses by taking into account the effect of solid-state phase transformation was developed. Using a simple bead-on-plate model, the influence of solid-state phase transformation on residual welding stresses in a 2.25Cr1Mo steel TIG welded plate was studied. The early simulation results suggest that solid-state phase transformations drastically reduce the longitudinal tensile stress in the weld and the heat-affected-zone, although it is also found that such phase transformation adversely increases the transverse residual stress in the region.

Since multi-pass welded components are more commonly utilized in practice, it is necessary to further look into the stress state of such components. Moreover, further work dealing with other materials rather than low carbon alloyed steels and combining the residual welding stresses with local damage and fracture mechanics also deserves further attention.

Acknowledgements

The authors would like to thank Mr. Nawafune and Mr. Kawahara of Osaka University for their helps to perform numerical simulations. This work was supported by the Open-Fund Research of State Key Laboratory of Advanced Welding and Joining, Harbin Institute of Technology, China and the Fundamental Research Funds for Central University (No. CDJZR12130036).

REFERENCES

[1] Handbook of residual stress and deformation of steel, ASM International, Ohio, USA, 2002, pp3–10.
[2] D. Deng, Mater. Des. **30(2)** (2009) 359.
[3] T. Inoue and Z. Wang, Mater. Sci. Technol. **1** (1985) 845.
[4] F.M.B. Fernandes, S. Denis and A. Simon, Mater. Sci. Technol. **1** (1985) 838.
[5] B. Talijiat, B. Radhakrishnnan and T. Zacharia, Mater. Sci. Eng. A **246** (1998) 45.
[6] D. Deng and H. Murakawa, Comput Mater. Sci. **37** (2006) 209.
[7] S.H. Kang and Y.T. Im, Metall Mater. Trans. A **36** (2005) 2315.
[8] S.H. Kang and Y.T. Im, Int. J. Mech. Sci. **49** (2007) 423.
[9] H. Murakawa, I. Oda, S. Ito, H. Serizawa and J. Kansai, Soc. N. A., Japan, No. 243, 2005, pp.67–70.
[10] H. Nishikawa, H. Serizawa and H. Murakawa, J Jpn Weld Soc **24**(2) (2005) 168.
[11] D. Radaj, Welding Residual Stresses and Distortion Calculation and Measurement-DVS, Düsseldorf, DVS, Verlag, 2003, 3-87155-791-9.
[12] M. Fujita, J. Kinugawa, A. Okada and T. Kasugai, National Institute for Materials Science, Tokyo, Japan, 2003. http://inaba.nims.go.jp/weld/
[13] G.J. Oliver, Fitting Parameters to Phase Transformation Kinetic Equations from CCT and TTT Diagram Data, Research Report, JWRI, Osaka University, 2002.
[14] M. Lusk and H.J. Jou, Metall. Mater. Trans. A **28** (1997) 287.
[15] G. Krauss, Principles of Heat Treatment of Steel, ASM International, Materials Park, Ohio, 1990, p.229.
[16] D. Deng and H. Murakawa, Comput. Mater. Sci. **43** (2008) 681.